eNeuro

Research Article: New Research
Sensory and Motor Systems

Hawkmoth Pheromone Transduction Involves G-Protein–Dependent Phospholipase Cβ Signaling

Anna C. Schneider,* Katrin Schröder,* Yajun Chang, Andreas Nolte, Petra Gawalek, and Monika Stengl

University of Kassel, Kassel 34132, Germany

Abstract

Evolutionary pressures adapted insect chemosensation to their respective physiological needs and tasks in their ecological niches. Solitary nocturnal moths rely on their acute olfactory sense to find mates at night. Pheromones are detected with maximized sensitivity and high temporal resolution through mechanisms that are mostly unknown. While the inverse topology of insect olfactory receptors and heteromerization with the olfactory receptor coreceptor suggest ionotropic transduction via odorant-gated receptor–ion channel complexes, contradictory data propose amplifying G-protein–coupled transduction. Here, we used in vivo tip-recordings of pheromone-sensitive sensilla of male *Manduca sexta* hawkmoths at specific times of day (rest vs activity). Since the olfactory receptor neurons distinguish signal parameters in three consecutive temporal windows of their pheromone response (phasic; tonic; late, long-lasting), respective response parameters were analyzed separately. Disruption of G-protein–coupled transduction and block of phospholipase C decreased and slowed the phasic response component during the activity phase of hawkmoths without affecting any other component of the response during activity and rest. A more targeted disruption of G_{α} subunits by blocking $G_{\alpha o}$ or sustained activation of $G_{\alpha s}$ using bacterial toxins affected the phasic pheromone response, while toxins targeting $G_{\alpha q}$ and $G_{\alpha 12/13}$ were ineffective. Consistent with these data, the expression of phospholipase Cβ4 depended on zeitgeber time, which indicates circadian clock-modulated metabotropic pheromone transduction cascades that maximize sensitivity and temporal resolution of pheromone transduction during the hawkmoth's activity phase. Thus, discrepancies in the literature on insect olfaction may be resolved by considering circadian timing and the distinct odor response components.

Key words: circadian clock; insect; olfaction

Significance Statement

Insect chemosensory transduction is typically thought to be ionotropic, but data from different insect species suggest that metabotropic olfactory signaling may occur, either alongside or instead of ionotropic mechanisms. Nocturnal moths, known for their extraordinarily sensitive pheromone-detecting olfactory receptor neurons, likely use metabotropic signal amplification. To overcome limitations of previous in vitro studies, we conducted tip-recordings of pheromone-sensitive sensilla in healthy hawkmoths at specific zeitgeber times (ZT). Disrupting G-protein and phospholipase Cβ signaling reduced sensitivity and altered response kinetics, revealing strict temporal control of transduction. Thus, contradictory findings in insect olfaction may be reconciled by considering diverse evolutionary pressures for distinct chemosensory signals in different species, ZT, and disparate odor response parameters.

Received Aug. 29, 2024; revised Dec. 2, 2024; accepted Dec. 16, 2024.

The authors declare no competing financial interests.

Author contributions: A.C.S., K.S., Y.C., A.N., P.G., and M.S. designed research; K.S., Y.C., A.N., and P.G. performed research; A.C.S., K.S., and Y.C. analyzed data; A.C.S., K.S., Y.C., and M.S. wrote the paper.

This work was supported by Deutsche Forschungsgemeinschaft RTG 2749/1 STE531/20-1 2.

*A.C.S. and K.S. contributed equally to this work.

Correspondence should be addressed to Anna C. Schneider at anna.c.schneider@uni-kassel.de.

Copyright © 2025 Schneider et al. This is an open-access article distributed under the terms of the Creative Commons Attribution 4.0 International license, which permits unrestricted use, distribution and reproduction in any medium provided that the original work is properly attributed.

Introduction

Both male and female nocturnal *Manduca sexta* hawkmoths express daily rhythms in their mating behavior, which are synchronized via species-specific pheromones that are released exclusively at night. Superimposed on this slow, nightly rhythm of pheromone

release, female moths emit their sex pheromone blend in fast pulses via oscillatory exposure of their abdominal pheromone glands (Sasaki and Riddiford, 1984; Tumlinson et al., 1989; Riffell et al., 2008; Schendzielorz et al., 2015). Depending on wing fanning frequencies, Lepidoptera males detect intermittent changes of the pheromone/odor blend at specific ultradian frequencies, e.g., up to 25 Hz for *Bombyx mori* and up to 5 Hz for *Lymantria dispar* (Loudon and Koehl, 2000; Bau et al., 2005; Nakata et al., 2024). The males detect the pheromone blend with long trichoid sensilla on their antenna, each of which is innervated by two olfactory receptor neurons (ORNs). One of the two ORNs specifically detects bombykal (BAL), the main sex pheromone component, the other ORN responds to other components of the pheromone blend (Sanes and Hildebrand, 1976; Altner and Prillinger, 1980; Keil and Steinbrecht, 1984; Kaissling et al., 1989; Keil, 1989; Tumlinson et al., 1989). The properties of ORNs are controlled by their endogenous circadian clocks, which results in maximum sensitivity and fastest pheromone pulse tracking at night, during the hawkmoth's activity phase (Dolzer et al., 2003; Schuckel et al., 2007; Flecke and Stengl, 2009; Flecke et al., 2010).

Pheromone-sensitive ORNs of moths are outstandingly sensitive with a dynamic range that covers several log units of pheromone concentrations [e.g., *M. sexta*, ≥4 log units (Marion-Poll and Tobin, 1992; Dolzer et al., 2003); *B. mori*, 6–7 log units (Kaissling and Priesner, 1970)]. They are flux detectors, tuned to resolve fast changes in pheromone concentration (Baker and Vogt, 1988; Marion-Poll and Tobin, 1992; Kaissling, 1998). Their sensitivity and electrical response kinetics depend on stimulus strength and duration. Even brief exposure of several milliseconds to low concentrations of pheromone molecules results in prolonged alternation of the ORN spiking response (Dolzer et al., 2003). The molecular mechanisms, which are responsible for their exceptional sensitivity and which can be adjusted by zeitgeber time (ZT) and stimulus intensity, are poorly understood, and contradictory findings for insect pheromone/odor transduction cascades have been reported, even in the same species and for the same odorants (Nakagawa and Vosshall, 2009; Stengl, 2010, 2017; Stengl and Funk, 2013; Wicher and Miazzi, 2021).

Insect olfactory receptors (ORs) are seven-transmembrane (7TM) molecules with inverse topology and not related to the G-protein–coupled 7TM ORs of vertebrates (Clyne et al., 1999; Gao and Chess, 1999; Vosshall et al., 1999; Krieger et al., 2002, 2003; Benton et al., 2006; Lundin et al., 2007). In *Drosophila melanogaster*, ORs heteromerize with a distantly related but conserved inverse 7TM molecule, Or83b, the olfactory receptor coreceptor (Orco; Vosshall et al., 1999; Vosshall and Hansson, 2011). While an ionotropic mechanism was suggested for pheromone transduction in *B. mori* and both an ionotropic and mixed ionotropic and metabotropic transduction cascade for general odor detection in *D. melanogaster* (Sato et al., 2008; Wicher et al., 2008), no evidence for OR–Orco-dependent ionotropic pheromone transduction was found in *M. sexta* (Nolte et al., 2013, 2016). In *D. melanogaster*, OR–Orco complexes in heterologous expression systems constitute odorant-gated, nonspecific cation channels with slow-gating kinetics and a reversal potential ∼0 mV (Sato et al., 2008; Wicher et al., 2008). In contrast, in *M. sexta*, the first ion channel that activates after pheromone application is a transient Ca^{2+} channel with rapid kinetics that opens and closes in <100 ms. The resulting pheromone-dependent current resembles the inositol trisphosphate (IP_3)- or diacyl glycerol (DAG)-dependent currents that are reminiscent of TRP ion channel family-dependent currents (Stengl et al., 1992; Stengl, 1993, 1994; Gawalek and Stengl, 2018; Dolzer et al., 2021). Thus, in hawkmoths, pheromone transduction was suggested to employ a metabotropic G-protein–coupled cascade that activates phospholipase Cβ (PLCβ), which allows strong signal amplification and a flexible, adjustable dynamic range (Stengl, 2010).

In contrast to most of the previous research on insect odor/pheromone transduction cascades, here, we used in vivo experiments in healthy *M. sexta* hawkmoths to challenge the hypothesis of metabotropic PLCβ -dependent pheromone transduction. We combined tip-recordings of pheromone-sensitive long trichoid sensilla with pharmacology in search for circadian modifications of pheromone transduction that are not directly mediated by light levels. We compared the ORN responses with BAL stimulation, where we applied synthetic BAL to the olfactory sensilla via an antenna-directed air stream, at the end of the hawkmoth's activity phase at ZT 1–3 to the response at the resting phase at ZT 9–11. The BAL-elicited spiking response consists of three consecutive components with distinct firing patterns and durations. Each of the components carries different information of the pheromone signal (Dolzer et al., 2003; Nolte et al., 2013, 2016). Changes in pheromone concentration are encoded only by the latency and spike frequency of the first component, the phasic response (∼10 spikes; Dolzer et al., 2003). Thus, a comprehensive data analysis of the distinct components of the pheromone/odor response is necessary because, while being conserved across insects, their distinct kinetics indicate different underlying mechanisms of insect olfaction (Kaissling, 1986, 1987; Dolzer et al., 2003; Nolte et al., 2013, 2016; Stengl and Funk, 2013; Stengl, 2017). Therefore, we carefully distinguished response parameters, both in terms of response component and ZT.

Materials and Methods

Animals. For all experiments, we used 2- to 3-d-old adult male *M. sexta* (Lepidoptera, Sphingidae) hawkmoths from the breeding and rearing colonies at the University of Kassel. Animals were raised on an artificial diet and kept under long-day conditions (L:D; 17:7 h) at 24–26°C and relative humidity of 40–60%. After pupation, males and females were separated, and males were housed isolated from pheromones. Animals were fed and raised as described in Gawalek and Stengl (2018). In brief, caterpillars were fed with an artificial diet modified after Bell and Joachim (1976); adult moths were fed with sucrose solution.

Solutions. Salts for ringer solutions were purchased from Merck. Bacterial toxins, U73122 and U73343, were purchased from Sigma-Aldrich. All other chemicals were obtained from Sigma, unless stated otherwise. All substances were HPCL grade, unless noted otherwise.

Ringer solutions were prepared as described previously (Gawalek and Stengl, 2018). In brief, sensillum lymph ringer (SLR) contained the following (in mM), 172 KCl, 3 $MgCl_2$, 1 $CaCl_2$, 25 NaCl, 10 HEPES, and 22.5 glucose, pH 6.5, and adjusted to 475 mOsmol/kg with glucose. Hemolymph ringer (HLR) contained the following (in mM), 6.4 KCl, 12$MgCl_2$, 1 $CaCl_2$, 12 NaCl, 10 HEPES, and 340 glucose, pH 6.5, and adjusted to 450 mOsmol/kg with glucose.

Synthetic bombykal (BAL; E,Z-10,12-hexadecadienal; gift from J. H. Tumlison, Center for Medical, Agricultural and Veterinary Entomology) was prepared as stock solution of 100 µg/ml in *n*-hexane and stored at −80°C until use.

As general inhibitor of G-proteins, we used 10^{-5} M GDP-β-S (10^{-2} M stock solution dissolved in DMSO, Jena Bioscience) in SLR. For further discrimination between G-protein subunits, we used the following bacterial toxins. Pertussis toxin (pTox; 500 ng/500 µl solution in SLR, stored at 4°C until use) is a specific inhibitor of $G_{\alpha o}$, a subunit that usually inhibits adenylyl cyclase and therefore results in increases in cAMP levels (Mangmool and Kurose, 2011), in *D. melanogaster* (Hopkins et al., 1988). In insect antennae, pTox has been shown to inhibit the pheromone-dependent IP_3 production (Boekhoff et al., 1990, 1993). Cholera toxin (cTox; purity ≥ 90%, 5 µg/500 µl solution in SLR, stored at 4°C until use) constitutively activates $G_{\alpha s}$, which activates adenylyl cyclase and leads to sustained increases in cAMP levels, also in insect antennae (Boekhoff et al., 1993; Deng et al., 2011). *Pasteurella multocida* toxin (pmTox; 500 ng/500 µl solution dissolved in SLR, stored at −20°C until use) activates $G_{\alpha q}$ and the $G_{\alpha i/o}$ subgroup in vertebrates, resulting in decreased cAMP and increased IP_3 levels (Surguy et al., 2014; not yet tested in insects). For disruption of phospholipase C (PLC) signaling, we used the antagonist U73122 and its respective nonfunctional analog U73343 (both prepared as 10^{-2} M stock solution dissolved in DMSO and stored at −80°C until use), diluted to a final concentration of 10^{-5} M in SLR.

Electrophysiology. To investigate the molecular mechanisms of the pheromone signal transduction cascade, we performed long-term (hours to days) tip-recordings of the ORNs of single antennal long trichoid sensilla (Kaissling, 1995) at room temperature (20–23°C). Animals were fixed in a custom-made holder with tape, and the antenna was immobilized with dental wax (Boxing Wax, Kerr) near the base. To record from ORNs, we slipped the recording electrode over the clipped tip of one long trichoid sensillum, and we inserted the reference electrode into the clipped flagellum close to the annulus where the recording electrode was located. Electrodes were moved with manual micromanipulators (MMJ, Märzhäuser Wetzlar; Leitz, Leica Microsystems). Electrodes were pulled from thin-walled borosilicate glass capillaries (OD, 1.5 mm; ID, 1.17 mm, Harvard Apparatus) with a tip opening that both sealed well around the sensillum and fit the inside of the antenna (~1 µm). The opening of the cut flagellum around the reference electrode was sealed with electrode gel (GE Medical Systems Information Technology) to prevent dessiccation. The recording electrode was filled with SLR, and the reference electrode was filled with HLR. ORN activity was amplified 200-fold (custom build amplifier with 10^{12} Ω input impedance, or BA-03X, npi, or ELC-01MX, npi), low-pass filtered with a cutoff frequency of 1.3 kHz, digitized at 20 kHz with a Digidata (1200 or 1550A or 1550B, Molecular Devices), and saved for off-line analysis with pClamp 8 or 10 (Molecular Devices). We used pClamp to record the signal as high-pass filtered (150 Hz cutoff frequency) AC signal in addition to the unfiltered (DC) signal.

For BAL stimulation, 10 µl stock solution was loaded on filter paper (~1 cm^2), resulting in 100 ng BAL per filter paper. The solvent was allowed to evaporate and does not elicit responses from the BAL-sensitive ORN (Dolzer et al., 2003). Antenna-directed air streams for stimulation were set up according to previously described protocols (Nolte et al., 2013; Gawalek and Stengl, 2018). In brief, an odorless airstream was continuously blown over the antenna from a distance of ~5 cm to adapt antennal mechanoreceptors. The airstream could be passed through a cartridge containing the BAL loaded filter paper via TTL switching of solenoid valves. BAL stimulation consisted of periodic application of a 50 ms pulse at an interstimulus interval of 5 min to avoid desensitization and habituation (Dolzer et al., 2003). Recordings with SLR in the recording electrode served as controls, either with or without the addition of 0.1% DMSO, as specified. The addition of 0.1% DMSO to the SLR did not alter the recorded BAL response. Activators, inhibitors, or toxins were added to the SLR of the recording electrode.

To search for ZT-dependent effects, we recorded during the animal's late activity phase (ZT 1–3) and in the middle of its resting phase (ZT 9–11). In experiments involving G-protein or PLC signaling disruption, we recorded from different animals at the different ZTs and different interference conditions. Recording and periodic stimulation usually lasted for 120 min, with a few exceptions in the control recordings, which only lasted for ~70 min. In the toxin experiments, we did paired recordings of the same animal at the same ZTs on two consecutive days. For these experiments, we always filled the recording electrode with toxin SLR, obtained the control recordings on Day 1 immediately after attaching the electrode but before the toxins had any effect, and recorded on the same ZT on Day 2 without removing the electrodes in between. Here, we stimulated three times in the control recording and six times in the toxin recording.

Tissue collection, RNA extraction, and cDNA synthesis. We collected antennal tissue from isolated cultures of 2-d-old males. At each ZT 1, ZT 9, and ZT 17, we collected three samples with eight antennae per sample. All samples were immediately frozen in liquid nitrogen and stored at −80°C for RNA extraction. Total RNA was isolated using TRIzol Reagent (Invitrogen) according to the manufacturer's protocol. The quality of the RNA was assessed by gel electrophoresis. The

concentration and purity of RNA were detected using NanoDrop ND-1000 spectrophotometer (Thermo Fisher Scientific). $OD_{260/280}$ ratios of all samples were 1.8–2.0. The first-strand complementary DNA (cDNA) was synthesized with 1 µg of total RNA for each sample using the PrimeScript RT reagent Kit with gDNA Erase (Takara Bio) according to the manufacturer's instructions and stored at −20°C until use.

Phylogenetic analysis of PLCβ *from* M. sexta *and other species.* Since the *PLCβ* gene is not annotated clearly in the genome of *M. sexta*, we utilized the coding sequences (cds) of the *PLCβ* genes from *D. melanogaster* and *B. mori*. We identified two highly similar genes in *M. sexta* as candidate *PLCβ1* (*Plc21C*; gene ID: LOC115440592) and *PLCβ4* (*norpA*; gene ID: LOC115451385) with BLAST analysis in the NCBI database. We downloaded the cds of these candidate genes and the *PLC-β* genes of other insects, *Homo sapiens* and *Mus musculus*. We translated the cds into protein sequences and performed sequence alignments using MEGA X (Kumar et al., 2018). The phylogenetic tree was constructed using the maximum likelihood method and Tamura-Nei model (Tamura and Nei, 1993), and node support was evaluated with 1,000 bootstrap replicates.

Real-time quantitative polymerase chain reaction (qPCR). qPCR was conducted to determine the expression of target genes (Table 1) at ZT 1, ZT 9, and ZT 17 of hawkmoth antennae with TB Green Premix Ex Taq II (Tli RNase H Plus, Takara Bio). Primers for each target gene were designed using the Primer-BLAST online program of NCBI (Table 1). *Ribosomal Protein S13* (*RPS13*; Fenske et al., 2018) and *Glyceraldehyde-3-Phosphate Dehydrogenase* (*G3PDH*; Mészáros and Morton, 1996; Adamo et al., 2016) were chosen as the reference genes to normalize the relative expression levels of each target gene. Agar gel electrophoresis, sequencing of PCR fragments, and subsequent qPCR showed that the expression levels of the reference genes in the antennae were stable at ZT 1, ZT 9, and ZT 17. In this study, all primers were used to amplify the target genes via PCR with cDNA. Following amplification, the PCR products were resolved by gel electrophoresis. Target bands were excised and purified using NucleoSpin Gel and PCR Clean-Up Kit (Macherey-Nagel). The purified DNA was subsequently sequenced using the Sanger method to verify the specificity of the amplified fragments.

The qPCR reaction program was 95°C for 30 s, followed by 40 cycles of 95°C for 5 s and 60°C for 30 s. For each gene and biological repeat there were three technical replicates. The amplification efficiency of all primers was 90–110%. The relative expression levels of these target genes were calculated according to the $2^{-\Delta\Delta Ct}$ method (Livak and Schmittgen, 2001).

Data analysis. For evaluation of pheromone responses, both the unfiltered (DC) and high-pass filtered signal (AC) were examined. Spikes were detected by a threshold search on the AC trace. The following pheromone response parameters of the ORN spike train were evaluated during the first second after BAL stimulation (Fig. 1*A*): latency of the first spike relative to the beginning of the DC pheromone response, phasic spike frequency as the average instantaneous frequency of the first six spikes (F_{6AP}), the number of spikes in a 1 s window (general G-protein and PLC disruption experiments), or 100 ms window [toxin experiments; #APs (early)], and sensillum potential amplitude (SPA). The SPA was measured as the maximal deflection of the transepithelial potential following the BAL stimulation. Furthermore, for analysis of response kinetics, all action potentials (APs) within the first second after BAL stimulation were counted and binned in 10 ms bins. For the late long-lasting pheromone response (LLPR) that persists over several minutes after pheromone stimulation, we counted the number of spikes in the 295 s before the next BAL stimulus (Fig. 1*B*).

In experiments involving G-protein or PLC signaling disruption, the time course of the responses to repeated stimulation varied across animals, presumably due to individual differences in the reaction to DMSO application in vivo or differences

Table 1. Forward and reverse primer sequences for target and reference genes. Asterisks indicate candidate reference genes.

Gene	Primer sequence (5′-3′)	Size (bp)	Reference
timeless	F: TTAAGCCGACCGTAGTGCTG R: CGTCTTCCGTCCATGTGTCT	120	-
$G_{\alpha o}$	F: AAGCTGCTGCTCCTTGGTGCT R: GGCGACGAGCGATTGAATAGTG	147	-
$G_{\alpha q}$	F: CATTCACGGGTCGGGTTACA R: CTCCGCCTTTTCTACGTTGG	151	-
$G_{\alpha s}$	F: AGTCGACCATCGTGAAGCAG R: TTGCACCGGTGATCGTAAGT	126	-
PLCβ1	F: CGACACCATAAGCCAGTCCA R: CGGTTTGCCGTCGGTTAAAT	115	-
PLCβ4	F: GATATGGATCAGCCCCTCGC R: AGTTCTACGCACCTGCATCC	137	-
*RPS13**	F: GTCTTGCCCCTGACCTACCT R: TGGCAGCACACTCTTTGTCT	173	(Fenske et al., 2018)
*G3PDH**	F: CGATTAAGGAACTTGAGGACG R: ATAAGGAAGCGGATGCAAGG	232	(Mészáros and Morton, 1996; Adamo et al., 2016)

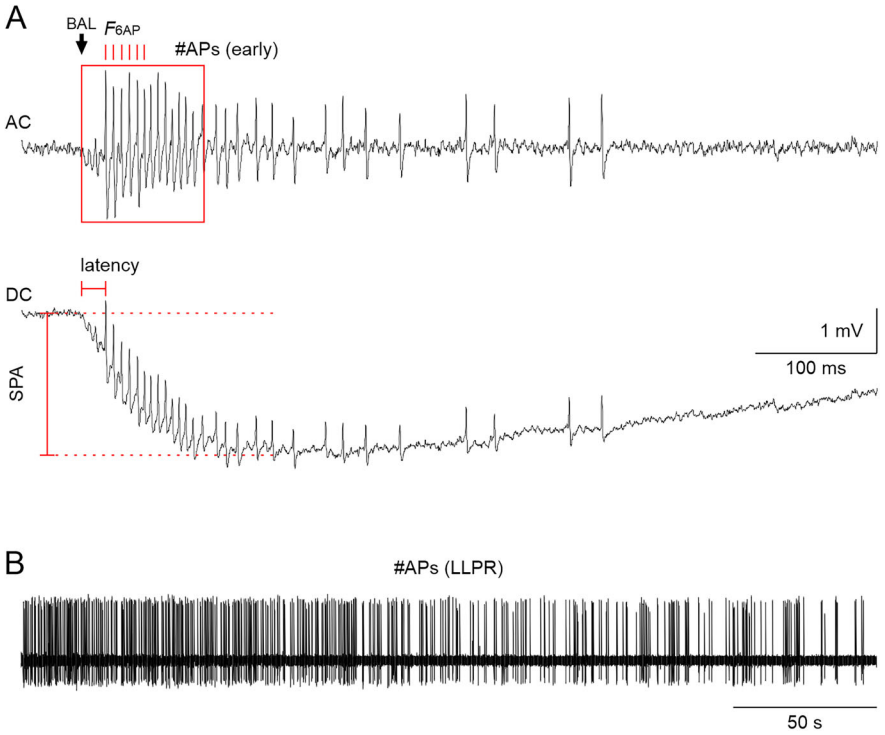

Figure 1. Quantification of the three phases of the pheromone response of hawkmoth long trichoid sensilla. The BAL-elicited spiking response consists of three consecutive spiking patterns (3 components) with distinct kinetics but variable duration (1) a phasic, high-frequency spiking response that lasts <100 ms (***A***), (2) a tonic spiking response with lower and more variable spiking frequency that lasts >100 ms (***A***), and (3) a late long-lasting spiking response (LLPR) that lasts seconds to minutes (***B***) (Dolzer et al., 2003; Nolte et al., 2016). ***A***, High-pass filtered (AC, top trace) and unfiltered (DC, bottom trace) recording of the sensillum potential with APs of the phasic–tonic ORN response to BAL. BAL stimulus: 50 ms, 10 µl of 0.1 mg/ml on 1 cm^2 filter paper; arrow: start of the BAL response. For the phasic response, we calculated the average instantaneous AP frequency of the first six APs (F_{6AP}, red ticks, top trace) of the BAL response. A combination of both phasic and part of the tonic response was evaluated as the number of APs in a 100 ms window starting at the onset of the BAL response [#APs (early), red box, top trace]. Latency (red horizontal marking, bottom trace) is the time from the beginning of the BAL response to the first AP. SPA is the amplitude from the baseline voltage before BAL stimulation to the negative peak (red vertical marking, bottom trace) (***B***) High-pass filtered recording of the LLPR. The LLPR was evaluated as the number of APs [#APs (LLPR)] in the 295 s before the next BAL stimulus, excluding the first 5 s after the BAL stimulus.

between individual sensilla. First effects were usually observed within 10–30 min after placement of the electrodes, but due to the in vivo recording method, the final concentration of the chemicals in the sensillum lymph was unknown. Therefore, we used linear fits to describe the change of each response parameter over the 120 min of stimulation. The slopes of the fits were used for quantification (Fig. 2*A*). Slopes that were not significantly different from zero (no significant change of the response over time, *t* test) were set to zero.

To quantify the changes of the kinetics of the spiking response to BAL stimulation, we created cumulative histograms of the binned data and fitted those histograms with the sigmoidal function as follows:

$$\mathrm{AP}(t) = \frac{\mathrm{AP}_{\max}}{1 + \exp\dfrac{t - t_{1/2}}{k}}, \tag{1}$$

where $\mathrm{AP}_{\max}$ is the cumulative number of spikes within 1 s after stimulation, $t_{1/2}$ is the time of the midpoint, and k is the slope factor (Fig. 2*B*). The fit parameters were used for quantification.

Statistics. Data were tested for normal distribution with the Shapiro–Wilk test and for equal variance with Levene's test. We used one-way ANOVA or repeated-measure (RM) ANOVA for normally distributed data with equal variance as indicated. If data were not normally distributed, we log-transformed the data or used ANOVA on ranks if transformation did not result in a normal distribution. For pairwise comparisons, we used Tukey's post hoc test for normally distributed and Dunn's post hoc test for non-normally distributed data. All tests were done in SigmaPlot (version 12, Systat Software).

Results

The response of antennal pheromone-sensitive trichoid sensilla to BAL stimulation was recorded in vivo in restrained, intact male hawkmoths at two ZTs: at the end of the activity phase (ZT 1–3) and in the middle of the resting phase (ZT 9–11).

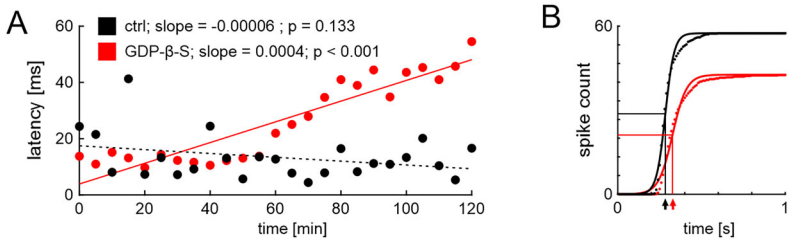

Figure 2. Illustration of the linear fit analysis of pheromone responses. ***A***, BAL stimuli were applied every 5 min in the 120-min-long tip-recordings of hawkmoth trichoid sensilla. For each animal and experimental condition [here, one control (black) and one GDP-β-S (red) animal], we generated a linear regression model for time and respective BAL response parameters (here, latency to the first AP after the onset of the BAL response) and used a *t* test to determine whether the slope of the fit significantly differed from zero (solid line) or not (dashed line). ***B***, To quantify the response kinetics to BAL stimulation, we binned the data of the first second after the BAL stimulus in 10 ms bins across all BAL stimulations for each animal. Each resulting cumulative histogram (dotted line) was fitted with a sigmoidal function (solid line) for quantification that yielded three fit parameters: maximum spike number (AP_{max}), time of the midpoint of the sigmoid ($t_{1/2}$; indicated by arrows at the *x*-axis), and slope of the midpoint (k). Depicted are examples of two animals.

Pharmacology was used to determine whether hawkmoth ORNs comprise G-protein–coupled pheromone receptors that activate PLCβ and whether this pathway is under the control of an ORN-based endogenous circadian clock to maximize sensitivity and temporal resolution of pheromone detection during the activity phase.

The pheromone response of ORNs consists of three components. The first component is fast and phasic and comprises <10 spikes (APs) which encode BAL concentration changes (Dolzer et al., 2003). It is characterized by regular, high-frequency spiking in a time window of $\leq$100 ms. The second component is tonic spiking at a lower and more variable frequency, which does not encode pheromone concentration changes but encodes signal duration within a limited range. It typically lasts several hundreds of milliseconds. This is followed by a pause and then the third component, the spiking of the LLPR, which can last seconds to minutes. The LLPR encodes neither quantity nor duration of the pheromone signal. It is distinct from the spontaneous activity before pheromone application and is hypothesized to encode a memory trace of the previous pheromone signal (Stengl, 2010).

General inhibition of G-proteins reduced the spike frequency and increased response latency of the phasic component of the BAL response during the activity phase but not during rest

To search for G-protein coupling in the pheromone transduction cascade, 10 µM GDP-β-S, an indiscriminative inhibitor of G-proteins, were infused via the tip-recording electrode into the pheromone-sensitive trichoid sensillum. The ORNs' neural responses to BAL stimulation were recorded with a nonadapting, periodic stimulation protocol (Dolzer et al., 2003) at two different ZTs in control and with GDP-β-S.

During the activity phase, blocking of G-protein–coupled processes reduced the frequency of the phasic response component (F_{6AP}), while the latency increased (Fig. 3*A*,*B*,*D*; ANOVA: Table 2; raw data: Extended Data Fig. 3-1). In contrast, GDP-β-S had no significant effect on F_{6AP} or latency during the resting phase (Fig. 3*B–D*; ANOVA: Table 2; raw data: Extended Data Fig. 3-1). However, response variability across animals increased in GDP-β-S at both ZTs over time, as indicated by the large increase in standard deviation (Fig. 3*B*,*C*). In addition, the kinetics of the response, i.e., rise and fall times to the maximum spike rate, were diminished with GDP-β-S during the activity phase but not at rest, as indicated by the larger slope factor *k* of the sigmoidal fits (Fig. 4; ANOVA: Table 3; raw data: Extended Data Fig. 4-1). GDP-β-S application did not have significant effects on any of the other response parameters at either ZT.

In conclusion, only the first component of the BAL response, which encodes stimulus concentration (F_{6AP}, latency), appears to be under the control of G-proteins. This metabotropic signaling changed with ZT.

Inhibition of PLC reduced the spike frequency of the phasic component of the BAL response at both ZTs while increasing response latency and decreasing SPA during the activity phase

In a complementary experiment, the PLC inhibitor U73122 was infused via the tip-recording electrode during the same ZTs as in the experiment above, where G-protein action was blocked. Infusion of U73343, a structurally similar but very weak inhibitor of PLC, served as the control. Overall, results were comparable with those obtained in GDP-β-S with some ZT-dependent differences (Fig. 5; ANOVA: Table 4; raw data: Extended Data Fig. 5-1).

During the activity phase, the inhibition of PLC significantly reduced F_{6AP}, increased latency, and reduced the SPA over time (Fig. 5*B*,*D*). In addition, the inhibition of PLC significantly reduced F_{6AP} over time during the resting phase (Fig. 5*C*,*D*). All other response parameters did not show significant differences at either ZT. Similarly to the experiments with GDP-β-S, response variability across animals increased in U73122 at both ZTs over time, as indicated by the large increase in standard deviation (Fig. 5*B*,*C*).

In conclusion, the inhibition of PLC, a downstream target of G-proteins, affected mainly the first component of the BAL response. Most of the effects were observed during the activity phase of the animals.

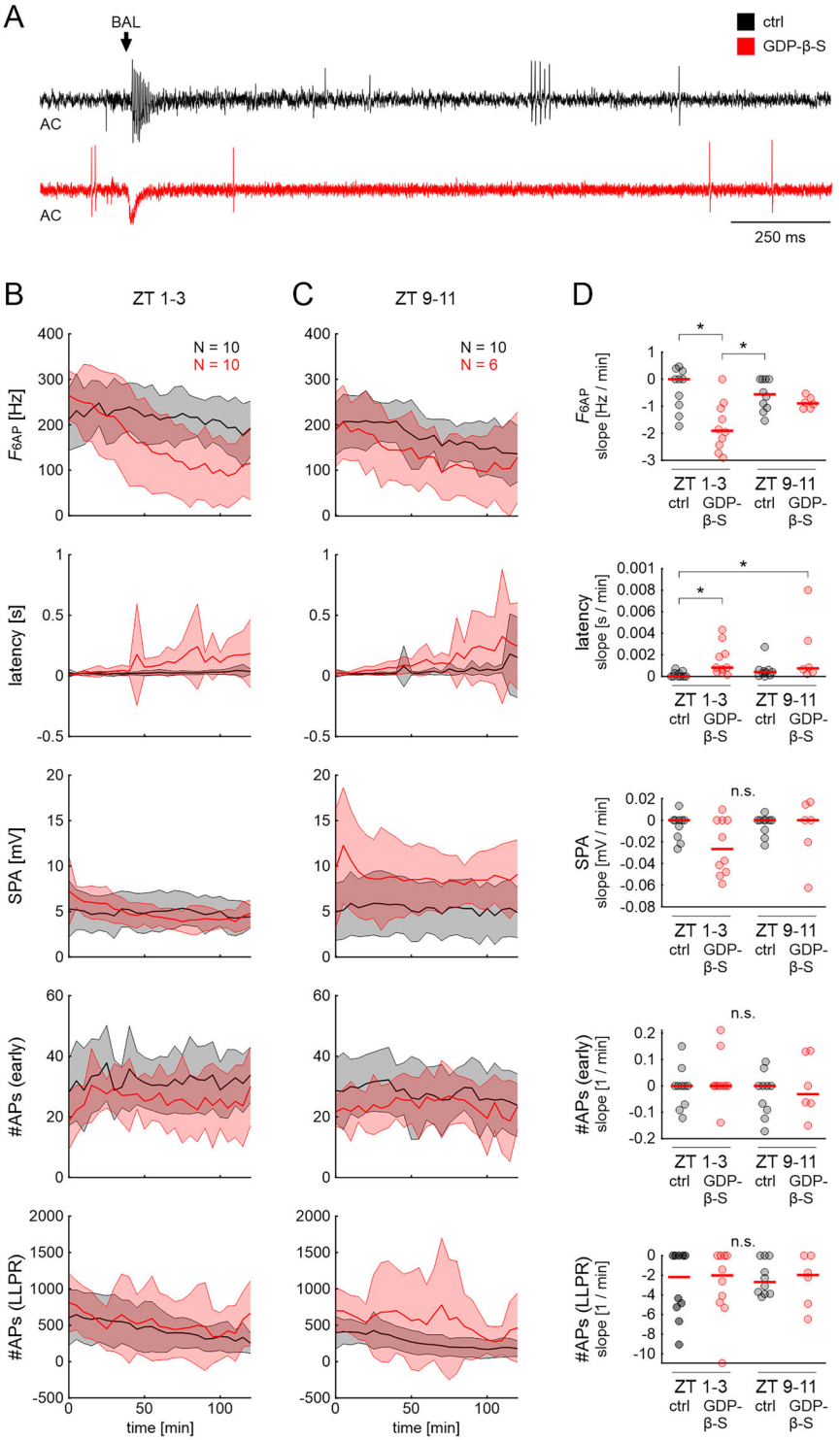

Figure 3. Inhibition of G-protein signaling of pheromone-sensitive ORNs by GDP-β-S decreased the phasic BAL response and increased response latency during the hawkmoth's activity phase. ***A***, Examples of high-pass filtered tip-recordings (AC) of ORN responses in control (ctrl, recording solution + DMSO, black) and with the G-protein antagonist GDP-β-S (dissolved in SLR + DMSO, red) at ZT 1–3, 100 min after the start of the recording. Arrow indicates the onset of BAL response. Response parameters (Fig. 1) during the moth's late activity phase (ZT 1–3; ***B***) and at rest (ZT 9–11; ***C***) in control and GDP-β-S. Data are shown as mean (line) ± standard deviation (shaded area). ***D***, One-way ANOVA results with appropriate post hoc test for multiple comparisons ($\alpha = 0.05$) for the slopes of BAL response parameters (see Materials and Methods and Fig. 2*A*). F_{6AP} slopes decreased significantly, and latency slopes increased significantly in GDP-β-S compared with control at the activity phase (ZT 1–3). No other parameters showed significant differences compared with control at either ZT. Dots show data for individual experiments; red lines indicate the mean. Raw data are provided in Extended Data Figure 3-1.

Table 2. One-way ANOVA results for BAL response parameters in control and GDP-β-S

N	Parameter	Normality	Variance	Test statistic	df	Res.	*p*
10	F_{6AP}	Pass	Pass	$F = 7.492$	3	32	**<0.001**
10	latency	Fail		$H = 13.975$	3		**0.003**
10	SPA	Pass	Fail	$H = 3.497$	3		0.321
10	#APs (early)	Pass	Pass	$F = 0.546$	3	32	0.654
10	#APs (LLPR)	Fail		$H = 0.203$	3		0.977

If tests for normality (Shapiro–Wilk) or equal variance (Levene) failed, results are for ANOVA on ranks. The four groups are ctrl ZT 1–3, GDP-β-S ZT 1–3, ctrl ZT 9–11, and GDP-β-S ZT 9–11. *p* values smaller than $\alpha = 0.05$ are printed in bold. *N*, number of animals; df, degrees of freedom; res: residual.

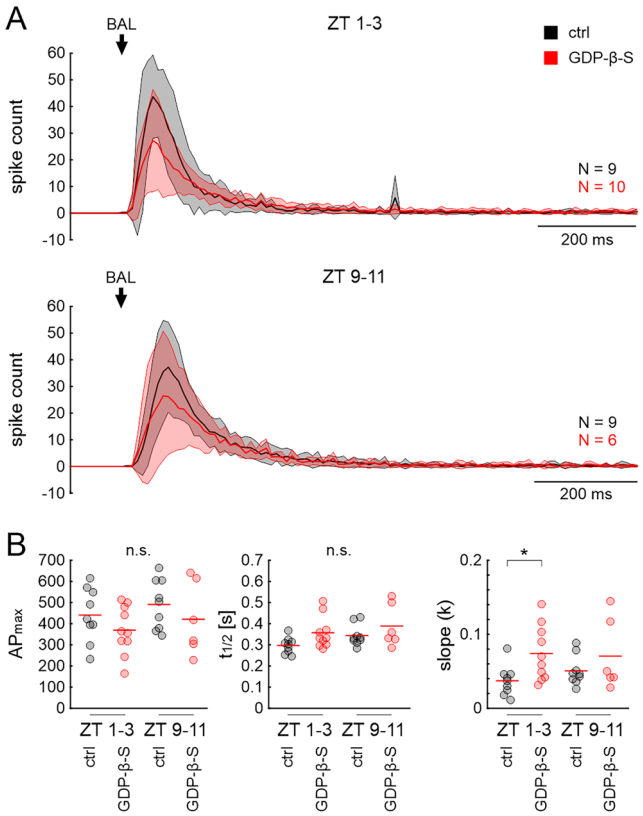

Figure 4. Inhibition of G-protein signaling changed kinetics of the ORN response to BAL stimulation during the activity phase. ***A***, Peristimulus time histograms (PTSH; 10 ms bins) of the first second of the ORN response to BAL stimulation in control (black) and in GDP-β-S (red). Data are shown as mean (line) ± standard deviation (shaded area). Arrow: onset of BAL response. ***B***, Fit parameters [total number of spikes in 1 s after onset of the BAL response (AP_{max}), time of the sigmoid midpoint ($t_{1/2}$), and slope (k) of the midpoint] of sigmoidal fits to the cumulative spike histograms (see Eq. 1, Materials and Methods, and Fig. 2*B*). One-way ANOVA with appropriate post hoc test ($\alpha = 0.05$) revealed a significantly steeper slope (*k* closer to zero) in control compared with GDP-β-S during the activity phase (ZT 1–3). Steeper slopes indicate faster rise and fall times of the spike count in the PTSHs. The total number of spikes and sigmoid midpoint were not significantly different. Dots show fit parameter values for individual experiments; red lines indicate the mean. Raw data are provided in Extended Data Figure 4-1.

Toxins targeting $G_{\alpha o}$ and $G_{\alpha s}$ reduced the spike frequency and increased the response latency of the phasic component of the BAL response during the activity phase

Thus far, the results indicated that G-protein signaling and activation of PLC were involved in the hawkmoth pheromone transduction cascade. Typically, PLC is activated by the αq subunit of G-proteins and increases IP_3 levels. Therefore, the bacterial toxins cTox, pTox, and pmTox were applied to specifically activate or inhibit different G_α subunits, which interferes with cAMP and IP_3 levels (see Materials and Methods). These experiments were done only during the hawkmoth's activity phase at ZT 1–3 because G-protein and PLC inhibition in the previous experiments were effective at those times. As with the chemicals before, toxins were applied to the sensillum via the recording electrode.

Both cTox and pTox application resulted in significant differences in the first and second component of the BAL response that were similar to the results obtained with GDP-β-S and U73122: activation of $G_{\alpha s}$ and inhibition of $G_{\alpha o}$ both decreased F_{6AP} and increased latency significantly (Fig. 6; ANOVA: Table 5; raw data: Extended Data Fig. 6-1). In addition, these toxins significantly reduced the number of spikes in the first and second component of the response [#APs (early)]. SPA and #APs (LLPR) were not altered. The application of pmTox did not have any significant effects (Fig. 6*B*).

Table 3. One-way ANOVA results for the fit parameters of the BAL response kinetics (Eq. 1)

N	Parameter	Normality	Variance	Test statistic	df	res.	*p*
10	AP_{max}	Pass	Pass	$F = 1.414$	3	30	0.258
10	$t_{1/2}$	Fail		$H = 7.243$	3		0.065
10	Log(slope)	Pass	Pass	$F = 3.212$	3	30	**0.037**

Data for slope were log-transformed to ensure normal distribution. If tests for normality (Shapiro–Wilk) or equal variance (Levene) failed, results are for ANOVA on ranks. The four groups are ctrl ZT 1–3, GDP-β-S ZT 1–3, ctrl ZT 9–11, and GDP-β-S ZT 9–11. *p* values smaller than $\alpha = 0.05$ are printed in bold. *N*, number of animals; df, degrees of freedom; res, residual.

In conclusion, toxins that are known to interfere with G-protein–dependent activation/disinhibition of adenylyl cyclase affected the BAL transduction in hawkmoths in the same way as PLC inhibition. Since pmTox did not result in significant changes of the BAL response, it remains to be studied whether pmTox affects any G-proteins in hawkmoths. The application of the toxins that increase cAMP concentration replicated the results that we obtained from G-protein and PLC inhibition.

Expression levels of PLCβ4 peaked during the activity phase

During the activity phase of the hawkmoth, but not during the resting phase, the disruption of G-proteins and PLC affected the pheromone response parameters that encode BAL concentration. Therefore, we examined whether these effects were caused by circadian changes in the antennal expression levels of $G_{\alpha o}$ or $G_{\alpha q}$, which activate PLCβ (increased IP_3 levels), or $G_{\alpha s}$, which activates adenylyl cyclase (increased cAMP levels). The expression levels of G_α subunits and PLCβ, which we found in the transcriptome of male hawkmoth antennae, were quantified with qPCR (Fig. 7). Phylogenetic analysis clustered the putative PLCβ candidate transcripts with those of *B. mori* (Extended Data Fig. 7-1; the nucleotide sequences of the genes are listed in Extended Data Fig. 7-2). Expression of the circadian clock gene *timeless* (*tim*) served as the positive control. Only *tim* and PLCβ4 (*norpA*) showed significantly different expression levels throughout the day, with higher expression levels during the activity phase (Fig. 7; Table 6). The expression of G_α subunits and PLCβ1 did not change.

Discussion

Chemosensory transduction is under strict circadian control in insects, and previous experiments in solitary nocturnal moths suggest that the transduction cascade differs between sleep and activity states (Zhukovskaya, 1995; Linn et al., 1996; Plautz et al., 1997; Krishnan et al., 1999; Page and Koelling, 2003; Rosén et al., 2003; Flecke et al., 2006, 2010; Merlin et al., 2007; Rymer et al., 2007; Gawalek and Stengl, 2018; Dolzer et al., 2021) In *D. melanogaster* ORNs, experimental data support an ionotropic odor transduction cascade in addition to cAMP-dependent metabotropic signaling in response to general odorants (Nakagawa and Vosshall, 2009; Wicher and Miazzi, 2021). In contrast, no evidence was found for OR–Orco-dependent ionotropic pheromone transduction in the hawkmoth *M. sexta*, but evidence accumulated for G-protein–coupled activation of PLCβ (Stengl, 2010; Nolte et al., 2013, 2016; Stengl and Funk, 2013).

Although the inverse topology of insect ORs raised doubts about potential G-protein coupling (Benton et al., 2006; Wistrand et al., 2006), and some physiological studies found no evidence for G-protein–dependent cascades (Sato et al., 2008; Yao and Carlson, 2010), several physiological and neuroanatomical findings in different insect species strongly suggest that metabotropic cascades are involved in insect odor/pheromone transduction (Breer et al., 1988, 1990; Boekhoff et al., 1990, 1993; Ziegelberger et al., 1990; Stengl, 1993, 1994, 2010; Laue et al., 1997; Wegener et al., 1997; Wetzel et al., 2001; Kalidas and Smith, 2002; Kain et al., 2008; Wicher et al., 2008; Chatterjee et al., 2009; Nakagawa and Vosshall, 2009; Boto et al., 2010; Grosse-Wilde et al., 2010; Deng et al., 2011; Stengl and Funk, 2013; Ignatious Raja et al., 2014; Fleischer et al., 2018; Wicher and Miazzi, 2021). Therefore, in this study, we combined pharmacological experiments, which disrupted metabotropic signaling through different subunits of G_α proteins and their target, PLCβ, with tip-recordings of pheromone-sensitive trichoid sensilla in intact, healthy hawkmoths. Our qPRC results corroborate the interpretation of the electrophysiological results and provide evidence for circadian control of BAL-dependent transduction cascades.

Two lines of evidence suggested that more than one class of G-proteins is involved in pheromone transduction: the increase in the variability of the response parameters when G-protein signaling was blocked and the differences in the effects between interference with general G-protein signaling and specific PLC signaling. These findings were supported by the experiments that specifically targeted the αs and αo subunits of G-proteins, indicating that G-protein activation and cyclic nucleotides are involved in the regulation of the ORN sensitivity to pheromones.

The highly sensitive pheromone transduction in moths is coupled to $G_{\alpha o}$ and PLCβ

Solitary nocturnal moth males have only a few weeks as adults to accomplish the challenging task of locating their species-specific females for mating. Thus, evolution equipped moths with an exquisitely sensitive sense of smell that apparently allows the detection of single pheromone molecules (Kaissling and Priesner, 1970; Kaissling, 1986). To do so, the system needs mechanisms for the reduction of noise in the form of other olfactory molecules and maximized odor-specific signal

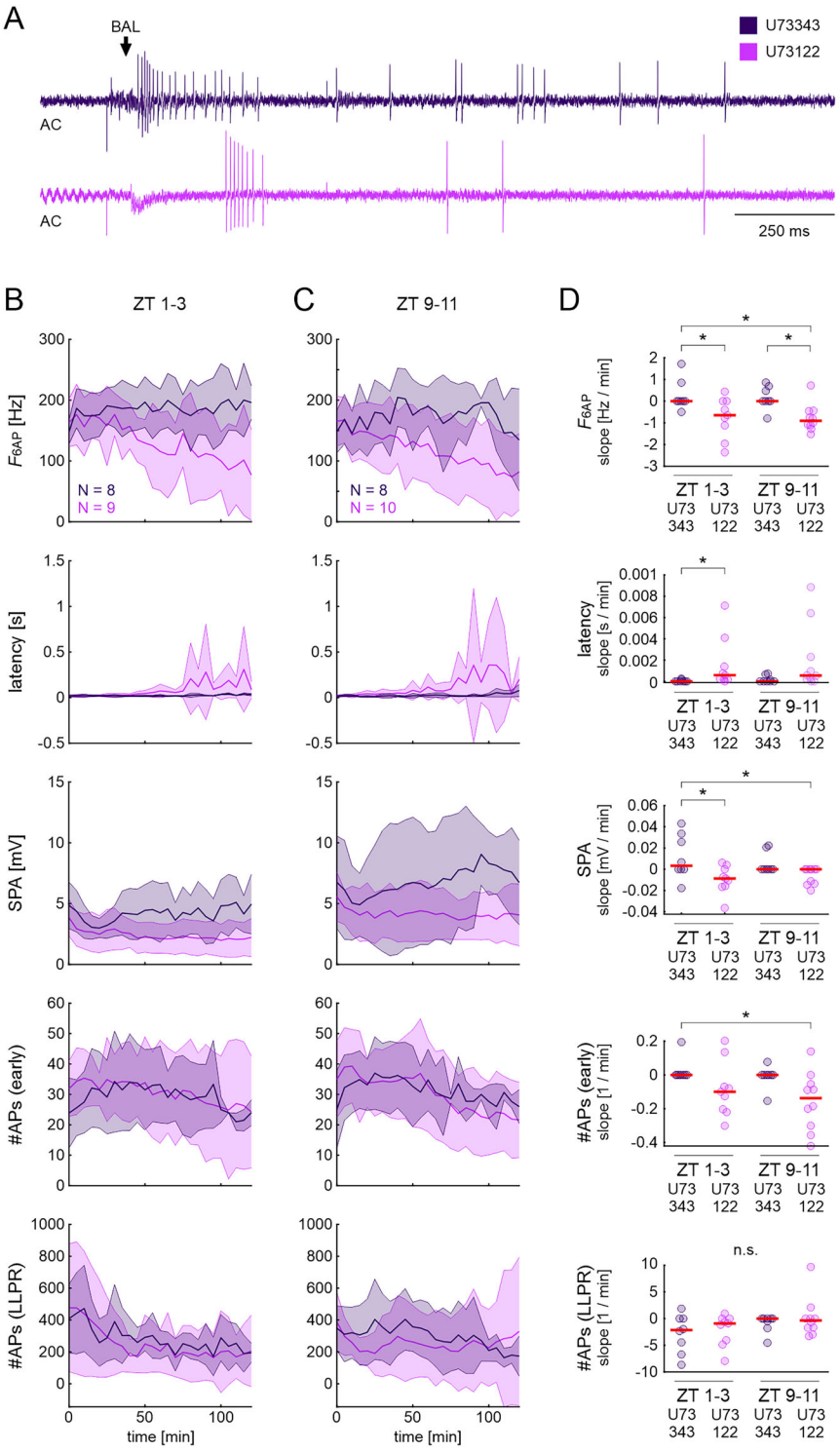

Figure 5. Inhibition of PLC of pheromone-sensitive ORNs with U73122 decreased the phasic BAL responses at both ZTs while decreasing SPA and increasing response latency only at ZT 1–3. ***A***, Example high-pass filtered (AC) tip-recordings of ORN responses in control (U73343, dark purple) and in PLC inhibitor (U73122, light purple) at ZT 1–3, 100 min. The arrow indicates the onset of the BAL response. Response parameters (Fig. 1) during the activity phase (ZT 1–3; ***B***) and at rest (ZT 9–11; ***C***) in control and U73122. Data are shown as mean (lines) ± standard deviation (shaded areas). ***D***, One-way ANOVA results with appropriate post hoc test for multiple comparisons ($\alpha = 0.05$) for the slopes of BAL response parameters (see Materials and Methods and Fig. 2*A*). Compared with controls, F_{6AP} slopes decreased at both ZTs in U73122, but SPA and latency slopes increased only at the activity phase (ZT 1–3). Other BAL response parameters showed no significant differences between control and U73122 at either ZT. Dots show data of individual experiments; red lines indicate the mean. Raw data are provided in Extended Data Figure 5-1.

Table 4. One-way ANOVA results for BAL response parameters in control (U73343) and U73122

N	Parameter	Normality	Variance	Test statistic	df	res.	*p*
10	F_{6AP}	Pass	Pass	$F = 5.447$	3	31	**0.004**
10	Latency	Fail		$H = 12.187$	3		**0.007**
10	SPA	Pass	Pass	$F = 4.493$	3	31	**0.010**
10	#APs (early)	Pass	Fail	$H = 10.327$	3		**0.016**
10	#APs (LLPR)	Pass	Pass	$F = 1.558$	3	31	0.219

If tests for normality (Shapiro–Wilk) or equal variance (Levene) failed, results are for ANOVA on ranks. Groups are ctrl ZT 1-3, U73122 ZT 1-3, ctrl ZT 9-11, and U73122 ZT 9-11. *p* values smaller than $\alpha = 0.05$ are printed in bold. *N*, number of animals; df, degrees of freedom; res, residual.

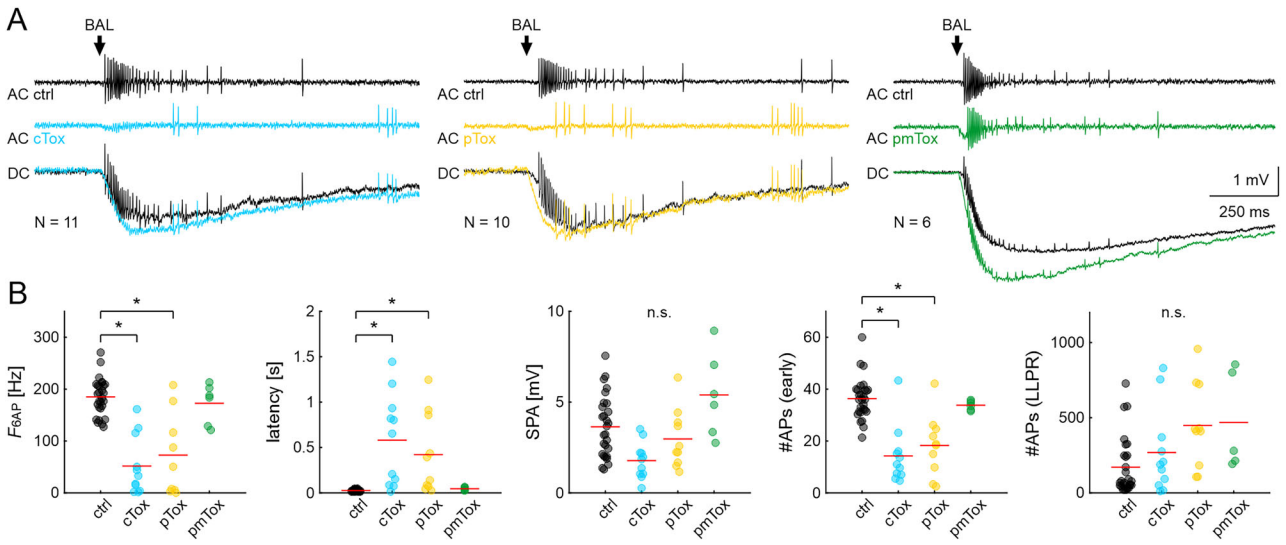

Figure 6. Responses to BAL stimulation at ZT 1–3 were affected by toxins that target $G_{\alpha s}$ or $G_{\alpha o}$ subunits. ***A***, Examples of tip-recordings from ORNs with BAL stimulation in control (black), with cTox (blue), pTox (yellow), and pmTox (green); repeated measures of one animal shown for each toxin. AC: high-pass filtered recording to highlight AP response; DC: unfiltered SPA with APs; Arrow: onset of the BAL response. ***B***, Quantification with one-way RM ANOVA with appropriate post hoc test for multiple comparisons ($\alpha = 0.05$) of the same parameters as in Figure 3 and Figure 5. During the activity phase (ZT 1–3), the frequency of the phasic BAL responses (F_{6AP}) and the number of APs during the first 100 ms of the response [#APs (early)] decreased in cTox (blue; sustained activation of $G_{\alpha s}$) and pTox (yellow; inhibition of $G_{\alpha o}$), while response latency increased significantly. The effect of pmTox (green; constitutive activation of $G_{\alpha 12/13}$, $G_{\alpha i}$, and $G_{\alpha q}$) was not different from control. Raw data are provided in Extended Data Figure 6-1.

Table 5. One-way RM ANOVA results for BAL response parameters in control and bacterial toxins at ZT 1–3

N	Parameter	Normality	Variance	Test statistic	df	res.	*p*
28	F_{6AP}	Pass	Pass	$F = 26.611$	3	23	**<0.001**
28	Log(latency)	Pass	Pass	$F = 26.606$	3	25	**<0.001**
28	SPA	Pass	Pass	$F = 1.996$	3	24	0.142
28	#APs (early)	Pass	Pass	$F = 22.252$	3	24	**<0.001**
28	#APs (LLPR)	Pass	Pass	$F = 3.726$	3	23	**0.026**

Values for latency were log-transformed to ensure equal variance. Groups are ctrl, pTox, cTox, pmTox. *p* values smaller than $\alpha = 0.05$ are printed in bold. *N*, number of animals; df, degrees of freedom; res, residual.

amplification. Patch-clamp experiments in primary cell cultures of *M. sexta* ORNs revealed the activation of three consecutive pheromone-dependent ionic currents with physiologically low concentrations of pheromone stimuli (Stengl, 1993, 1994). First, a rapid, transient, pheromone-dependent Ca^{2+} inward current activates and declines in <100 ms after the start of the pheromone response. Second, apparently based on the resulting increase in intracellular Ca^{2+}, a slower Ca^{2+}-gated, non-specific cation current activates, which underlies the slower kinetics of the second component of the pheromone response. Third, a protein kinase C -dependent, slow, nonspecific cation current activates that persists for several seconds and underlies the third component of the pheromone response (Stengl, 2010). Since initially activated Ca^{2+}-channel of the transduction cascade functions as a "yes-or-no trigger" for subsequent Ca^{2+}-dependent amplification steps, it both obliterates noise of previous processes and amplifies the signal via Ca^{2+}-dependent mechanisms.

The properties of that first Ca^{2+}-channel are different from those of the OR–Orco cation channels of *B. mori* or *D. melanogaster* (Sato et al., 2008; Wicher et al., 2008), so that OR–Orco-dependent ionotropic signaling seems unlikely

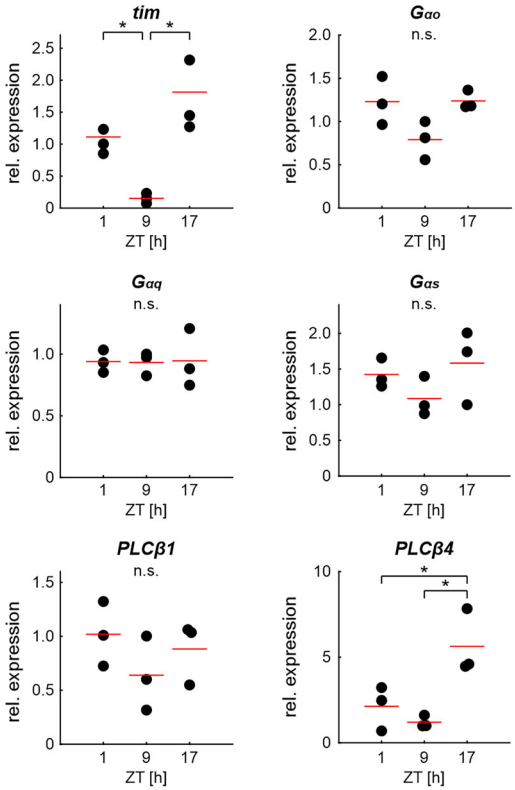

Figure 7. Relative expression levels of mRNA for G-proteins, PLCβ, and the circadian clock protein timeless (*tim*) in male hawkmoth antenna at different ZTs. qPCR revealed that mRNA levels of *PLCβ4* peaked significantly at the beginning of the activity phase at ZT 17. $G_{\alpha o}$, $G_{\alpha q}$, $G_{\alpha s}$, and *PLCβ1* did not change throughout the day. The mRNA of the cycling circadian clock protein timeless (*tim*) served as the positive control. Dots indicate values for biological replicates; each biological replicate contains extracts from eight antennae and three technical repeats. Red lines depict the mean. One-way ANOVA with appropriate post hoc test for pairwise comparisons ($\alpha = 0.05$). The phylogenetic tree for PLCβ is provided in Extended Data Figure 7-1. Nucleotide sequences of the genes are provided in Extended Data Figure 7-2.

Table 6. One-way ANOVA results for gene expression levels at ZT 1, ZT 9, and ZT 17

N	Gene	Normality	Variance	Test statistic	df	res.	*p*
3	*tim*	Pass	Pass	$F = 14.889$	2	6	**0.005**
3	$G_{\alpha o}$	Pass	Pass	$F = 4.276$	2	6	0.070
3	$G_{\alpha q}$	Pass	Pass	$F = 0.005$	2	6	0.995
3	$G_{\alpha s}$	Pass	Fail	$F = 1.479$	2	6	0.301
3	PLCβ1	Pass	Pass	$F = 1.137$	2	6	0.381
3	PLCβ4	Pass	Pass	$F = 9.001$	2	6	**0.016**

p values smaller than $\alpha = 0.05$ are printed in bold. *N*, number of animals; df, degrees of freedom; res, residual.

in *M. sexta* pheromone transduction (Nolte et al., 2013, 2016). Rather, the channels that give rise to at least the first two of the three consecutive ionic currents of the pheromone response in *M. sexta* seem to belong to the TRPC superfamily of TRP channels that are highly permeable to Ca^{2+}, which were originally described in the similarly highly sensitive phototransduction cascade of *D. melanogaster* (Hardie and Minke, 1992; Gawalek and Stengl, 2018). It was discovered only recently that TRPCs are not only linked to PLCβ activation but can also be directly gated by $G_{i/o}$ proteins (Jeon et al., 2020; Zhu, 2023). Whether this is true for the antennal TRPs of *M. sexta* remains to be examined.

In contrast to the first component, only the late, long-lasting third component of the pheromone response was linked to Orco in *M. sexta*. Therefore, a solely ionotropic mechanism of pheromone transduction, that is based on a pheromone-gated OR–Orco, is unlikely because the Orco channel does not open during the first phase of the pheromone response. It rather suggests cGMP-dependent and/or voltage-dependent Orco gating (Nolte et al., 2013, 2016).

The findings described in the current study are consistent with localization and functional analyses of G-protein subunits and PLCβ in different insect antennae. In antennae of *D. melanogaster*, RT-PCR reported the expression of six G_α subunits (G_s, G_i, G_q, G_o, G_f, and concertina) in addition to different G_β and G_γ subunits (Boto et al., 2010). There, G_s, G_i, and G_q are located in the cilia of ORNs, suggesting coupling to ORs (Kain et al., 2008; Boto et al., 2010). Different physiological and behavioral assays, in combination with molecular genetics, demonstrated that $G_{\alpha o}$ or $G_{\alpha q}$ signaling is used in odor

detection in *D. melanogaster* (Kalidas and Smith, 2002; Kain et al., 2008; Chatterjee et al., 2009; Ignatious Raja et al., 2014). In contrast, Yao and Carlson (2010) reported in an extensive study that $G_{\alpha q}$ and $G_{\gamma 30A}$ are involved in CO_2 detection through gustatory receptors, but not in OR-mediated odor signaling of antennal basiconic sensilla.

Regarding moths, $G_{\alpha o}$, $G_{\alpha q}$, and $G_{\alpha s}$ are expressed and localized in adult antennae of *B. mori* (Miura et al., 2005). In *Antheraea pernyi*, $G_{\alpha q}$ was found in homogenates of the antennal ciliary fraction and, by electron-microscopic studies, was detected in cilia of pheromone-sensitive trichoid sensilla. Hence, it is likely that $G_{\alpha q}$ is involved in pheromone detection in *A. pernyi* by coupling to ORs (Laue et al., 1997).

Furthermore, the pheromone-dependent fast, transient rises of IP_3 in homogenates of moth and cockroach antennae are consistent with the pheromone-dependent activation of PLCβ during the first component of the pheromone response (Breer et al., 1990; Boekhoff et al., 1993). Since pheromone-dependent rises in IP_3 levels are decreased by interfering with $G_{\alpha o}$ through pTox in the antennae of insects (Boekhoff et al., 1990), it is likely that, consistent with current data in hawkmoths and our results presented here, pheromone receptors in moths use $G_{\alpha o}$-dependent activation of PLCβ. It remains to be tested in detail whether and how pheromone transduction of different insect ORs couple directly to G-proteins and their respective target, PLCβ, or to other enzymes such as adenylyl cyclases.

In *D. melanogaster* and other insect species, members of the cAMP signaling cascades, or receptors coupled to cAMP signaling, have been found in the antennae (Schendzielorz et al., 2012, 2015; Thamm et al., 2017; J. Li et al., 2020, Y. Li et al., 2024). They were located in ORNs, by either demonstrating the respective gene expression with molecular genetic tools or by morphological assays with immunocytochemistry. Rises in cAMP were reported after odor stimulation and mutations of the cAMP cascade results in defects in olfaction-dependent behavior, which suggests that at least some specific ORs are relying on $G_{\alpha s}$-dependent activation of adenylyl cyclases in *D. melanogaster* (Wicher et al., 2008; Deng et al., 2011; Wicher and Miazzi, 2021).

The discrepancies in reports of insect olfaction could stem from inconsistent experimental conditions between the different studies. Conclusions from measurements of different sensillum types and ORNs are often generalized and not distinguished in different or even the same species. Additionally, odorant concentrations and stimulus durations differ vastly between publications. Furthermore, the intracellular Ca^{2+} concentrations in the recorded ORNs are not controlled and would affect ion channel availability for odor-dependent activation (Stengl, 2010; Stengl and Funk, 2013). As we demonstrated here, interference with pheromone transduction cascades depended on ZT and mostly affected the phasic component of the pheromone response. This and previous studies indicate that the three components of the response are mediated by distinct mechanisms of the transduction cascade, and failure to address these components separately could obscure G-protein actions that seem to act mostly on the first component. Very likely, careful planning and comparative analysis of experiments across species will show that there are several redundant transduction mechanisms for insect ORs, depending on the different physiological needs of the respective insect.

In summary, our physiological data from in vivo recordings of hawkmoth trichoid sensilla are consistent with pheromone receptor-dependent activation of $G_{\alpha o}$, which causes activation of PLCβ4 and therefore increases of IP_3 and diacylglycerol levels. Although BAL receptors in hawkmoth have the same inverse 7TM topology as ORs in other insects (Grosse-Wilde et al., 2006, 2007; Wicher et al., 2017), our results indicate direct or indirect coupling to G-protein–dependent amplification cascades, as shown for insect gustatory receptors and ionotropic receptors (Wetzel et al., 2001; Ishimoto et al., 2005; Nakagawa et al., 2005; Ueno et al., 2006; Stengl, 2010; Yao and Carlson, 2010). It seems that, in hawkmoths, there are several redundant or interdependent transduction cascades that guarantee the reliable, highly sensitive pheromone transduction, which depends on odor stimulus strength, duration, time course, and time of day, as well as on intracellular second messengers that vary across the day (Stengl, 2010; Stengl and Funk, 2013; Stengl and Schröder, 2021). It remains to be studied if and how receptors in ORNs and even in the non-neuronal support cells interact during pheromone and odor transduction.

Peripheral circadian clocks orchestrate olfaction-dependent behavioral rhythms via circadian control of chemosensory responsiveness

Nocturnal male moths are maximally responsive to pheromones during their activity phase in the scotophase (Linn et al., 1996; Rosén et al., 2003; Flecke et al., 2010). These rhythms in responsiveness are controlled by circadian clocks and therefore persist under constant conditions (Baker and Cardé, 1979; Rosén et al., 2003; Merlin et al., 2007). Similarly, females, guided by their own circadian clocks, release pheromones at night and peak release correlates with the males' search flight (Sasaki and Riddiford, 1984; Itagaki and Conner, 1988; Rosén, 2002). Mating success decreases if males and females are raised out of phase in different light/dark cycles (Silvegren et al., 2005). Both photoperiod and pheromone presence synchronize the mating behavior of moths by circadian modulation of female pheromone release and male pheromone sensitivity. How and where exactly this circadian modulation occurs in the male's olfactory system remains to be investigated further. Our results indicate that PLCβ4 is under circadian control and could be engaged in the heightened pheromone sensitivity, consistent with previous finding of circadian changes of IP_3 levels in hawkmoth antennae (Schendzielorz et al., 2015).

Circadian clocks generate rhythms with a cycle period of ∼24 h through positive feedforward and delayed negative feedback loops. These clocks are formed at the gene transcription level as transcriptional/translational feedback loop (TTFL) oscillators or at the posttranslational level as posttranslational feedback loop (PTFL) oscillators (Stengl and Schneider, 2024). The widespread and intertwined TTFL and PTFL oscillators sustain physiological homeostasis

(Stengl and Schneider, 2024) and occur not only in the central and peripheral nervous system but also in many organs throughout an organism (Plautz et al., 1997; Giebultowicz, 2000).

In response to food odors and pheromones, electroantennogram (EAG) recordings from *D. melanogaster*, the Mediterranean fruit fly *Ceratitis capitata*, and the cockroach *Rhyparobia maderae* show circadian rhythms (Krishnan et al., 1999; Page and Koelling, 2003; Merlin et al., 2007; Rymer et al., 2007; Sollai et al., 2018). Only targeted ablation of TTFL clock genes in the antenna, but not ablation of brain clocks, affected the circadian rhythms of EAGs in *D. melanogaster*, showing that the circadian oscillators in the antennae are necessary and sufficient for chemosensory rhythms (Tanoue et al., 2004). It is not well understood which mechanisms and which antennal cells control circadian rhythms in odor and pheromone sensitivity in insects, already at the periphery, and how these are synchronized to the central clock. Besides the ORNs in *M. sexta*, non-neuronal supporting cells and epithelial cells in the antennal sensilla express circadian clock genes with circadian rhythms, which suggests that many intertwined clocks and processes govern pheromone sensitivity in hawkmoths (Schuckel et al., 2007). Antennal genes that are involved in odorant binding and odorant clearance are rhythmically expressed (Claridge-Chang et al., 2001; McDonald and Rosbash, 2001; Ceriani et al., 2002; Merlin et al., 2007; Saifullah and Page, 2009; Jin et al., 2017; Dhungana et al., 2023). We could show for *M. sexta* that PLCβ4 expression depends on the time of day, which makes it a candidate for the circadian control of chemosensory sensitivity.

Concluding remarks

The results presented here add to the emerging view that the first stage of insect olfactory transduction is not solely realized through ionotropic receptors alone but apparently involves G-protein signaling cascades. While the investigation of olfactory receptors in heterologous expression systems allows for the elimination of confounding factors and the creation of a highly controllable environment, the use of an in vivo preparation ensures that all of the naturally occurring elements of signaling pathways are present. Furthermore, temporally separating the spiking response based on the known odorant attribute that is encoded in each response component instead of pooling the whole spike train mitigates the “failure of averaging”.

References

Adamo SA, Davies G, Easy R, Kovalko I, Turnbull KF (2016) Reconfiguration of the immune system network during food limitation in the caterpillar *Manduca sexta*. J Exp Biol 219:706–718.

Altner H, Prillinger L (1980) Ultrastructure of invertebrate chemo-, thermo-, and hygroreceptors and its functional significance. In: *International review of cytology* (Bourne GH, Danielli JF, eds), pp 69–139. New York: Academic Press.

Baker TC, Cardé RT (1979) Analysis of pheromone-mediated behaviors in male *Grapholita molesta*, the oriental fruit moth (Lepidoptera: Tortricidae). Environ Entomol 8:956–968.

Baker TC, Vogt RG (1988) Measured behavioural latency in response to sex-pheromone loss in the large silk moth *Antheraea polyphemus*. J Exp Biol 137:29–38.

Bau J, Justus KA, Loudon C, Cardé RT (2005) Electroantennographic resolution of pulsed pheromone plumes in two species of moths with bipectinate antennae. Chem Senses 30:771–780.

Bell RA, Joachim FG (1976) Techniques for rearing laboratory colonies of tobacco hornworms and pink bollworms1. Ann Entomol Soc Am 69:365–373.

Benton R, Sachse S, Michnick SW, Vosshall LB (2006) Atypical membrane topology and heteromeric function of *Drosophila* odorant receptors in vivo. PLoS Biol 4:e20.

Boekhoff I, Raming K, Breer H (1990) Pheromone-induced stimulation of inositol-trisphosphate formation in insect antennae is mediated by G-proteins. J Comp Physiol B 160:99–103.

Boekhoff I, Seifert E, Göggerle S, Lindemann M, Krüger B-W, Breer H (1993) Pheromone-induced second-messenger signaling in insect antennae. Insect Biochem Mol Biol 23:757–762.

Boto T, Gomez-Diaz C, Alcorta E (2010) Expression analysis of the 3 G-protein subunits, G_{α}, G_{β}, and G_{γ}, in the olfactory receptor organs of adult *Drosophila melanogaster*. Chem Senses 35:183–193.

Breer H, Boekhoff I, Tareilus E (1990) Rapid kinetics of second messenger formation in olfactory transduction. Nature 345:65–68.

Breer H, Raming K, Boekhoff I (1988) G-proteins in the antennae of insects. Naturwissenschaften 75:627–627.

Ceriani MF, Hogenesch JB, Yanovsky M, Panda S, Straume M, Kay SA (2002) Genome-wide expression analysis in *Drosophila* reveals genes controlling circadian behavior. J Neurosci 22:9305–9319.

Chatterjee A, Roman G, Hardin PE (2009) Go contributes to olfactory reception in *Drosophila melanogaster*. BMC Physiol 9:22.

Claridge-Chang A, Wijnen H, Naef F, Boothroyd C, Rajewsky N, Young MW (2001) Circadian regulation of gene expression systems in the *Drosophila* head. Neuron 32:657–671.

Clyne PJ, Warr CG, Freeman MR, Lessing D, Kim J, Carlson JR (1999) A novel family of divergent seven-transmembrane proteins: candidate odorant receptors in *Drosophila*. Neuron 22:327–338.

Deng Y, Zhang W, Farhat K, Oberland S, Gisselmann G, Neuhaus EM (2011) The stimulatory $G\alpha_s$ protein is involved in olfactory signal transduction in *Drosophila*. PLoS One 6:e18605.

Dhungana P, Wei X, Meuti M, Sim C (2023) Identification of CYCLE targets that contribute diverse features of circadian rhythms in the mosquito *Culex pipiens*. Comp Biochem Physiol Part D Genomics Proteomics 48:101140.

Dolzer J, Fischer K, Stengl M (2003) Adaptation in pheromone-sensitive trichoid sensilla of the hawkmoth *Manduca sexta*. J Exp Biol 206:1575–1588.

Dolzer J, Schröder K, Stengl M (2021) Cyclic nucleotide-dependent ionic currents in olfactory receptor neurons of the hawkmoth *Manduca sexta* suggest pull–push sensitivity modulation. Eur J Neurosci 54:4804–4826.

Fenske MP, Nguyen LP, Horn EK, Riffell JA, Imaizumi T (2018) Circadian clocks of both plants and pollinators influence flower seeking behavior of the pollinator hawkmoth *Manduca sexta*. Sci Rep 8:2842.

Flecke C, Dolzer J, Krannich S, Stengl M (2006) Perfusion with cGMP analogue adapts the action potential response of pheromone-sensitive sensilla trichoidea of the hawkmoth manduca sextain a daytime-dependent manner. J Exp Biol 209:3898–3912.

Flecke C, Nolte A, Stengl M (2010) Perfusion with cAMP analogue affects pheromone-sensitive trichoid sensilla of the hawkmoth *Manduca sexta* in a time-dependent manner. J Exp Biol 213:842–852.

Flecke C, Stengl M (2009) Octopamine and tyramine modulate pheromone-sensitive olfactory sensilla of the hawkmoth *Manduca sexta* in a time-dependent manner. J Comp Physiol A 195:529–545.

Fleischer J, Pregitzer P, Breer H, Krieger J (2018) Access to the odor world: olfactory receptors and their role for signal transduction in insects. Cell Mol Life Sci 75:485–508.

Gao Q, Chess A (1999) Identification of candidate *Drosophila* olfactory receptors from genomic DNA sequence. Genomics 60:31–39.
Gawalek P, Stengl M (2018) The diacylglycerol analogs OAG and DOG differentially affect primary events of pheromone transduction in the hawkmoth *Manduca sexta* in a zeitgebertime-dependent manner apparently targeting TRP channels. Front Cell Neurosci 12:218.
Giebultowicz JM (2000) Molecular mechanism and cellular distribution of insect circadian clocks. Annu Rev Entomol 45:769–793.
Grosse-Wilde E, Gohl T, Bouché E, Breer H, Krieger J (2007) Candidate pheromone receptors provide the basis for the response of distinct antennal neurons to pheromonal compounds. Eur J Neurosci 25:2364–2373.
Grosse-Wilde E, Stieber R, Forstner M, Krieger J, Wicher D, Hansson BS (2010) Sex-specific odorant receptors of the tobacco hornworm *Manduca sexta*. Front Cell Neurosci 4:22.
Grosse-Wilde E, Svatos A, Krieger J (2006) A pheromone-binding protein mediates the bombykol-induced activation of a pheromone receptor in vitro. Chem Senses 31:547–555.
Hardie RC, Minke B (1992) The *trp* gene is essential for a light-activated Ca^{2+} channel in *Drosophila* photoreceptors. Neuron 8:643–651.
Hopkins RS, Stamnes MA, Simon MI, Hurley JB (1988) Cholera toxin and pertussis toxin substrates and endogenous ADP-ribosyltransferase activity in *Drosophila melanogaster*. Biochim Biophys Acta 970:355–362.
Ignatious Raja JS, Katanayeva N, Katanaev VL, Galizia CG (2014) Role of $G_{o/i}$ subgroup of G proteins in olfactory signaling of *Drosophila melanogaster*. Eur J Neurosci 39:1245–1255.
Ishimoto H, Takahashi K, Ueda R, Tanimura T (2005) G-protein gamma subunit 1 is required for sugar reception in Drosophila. EMBO J 24:3259–3265.
Itagaki H, Conner WE (1988) Calling behavior of *Manduca sexta* (L.) (Lepidoptera: Sphingidae) with notes on the morphology of the female sex pheromone gland. Ann Entomol Soc Am 81:798–807.
Jeon J, Tian J-B, Zhu MX (2020) TRPC4 as a coincident detector of $G_{i/o}$ and $G_{q/11}$ signaling: mechanisms and pathophysiological implications. Curr Opin Physiol 17:34–41.
Jin S, Zhou X, Gu F, Zhong G, Yi X (2017) Olfactory plasticity: variation in the expression of chemosensory receptors in *Bactrocera dorsalis* in different physiological states. Front Physiol 8:672.
Kain P, Chakraborty TS, Sundaram S, Siddiqi O, Rodrigues V, Hasan G (2008) Reduced odor responses from antennal neurons of $G_q\alpha$, phospholipase Cβ, and *rdgA* mutants in *Drosophila* support a role for a phospholipid intermediate in insect olfactory transduction. J Neurosci 28:4745–4755.
Kaissling KE (1986) Chemo-electrical transduction in insect olfactory receptors. Annu Rev Neurosci 9:121–145.
Kaissling KE (1987) Stimulus transduction. In: *R. H. Wright lectures on insect olfaction* (Colbow K, ed), pp 1–190. Burnaby, BC: Simon Fraser University Press.
Kaissling KE (1995) Single unit and electroantennogram recordings in insect olfactory organs. In: *Experimental cell biology of taste and olfaction, current techniques and protocols* (Spielman I, Brand JG, eds), pp 361–386. Boca Raton, New York, Tokyo: CRC Press.
Kaissling KE (1998) Flux detectors versus concentration detectors: two types of chemoreceptors. Chem Senses 23:99–111.
Kaissling KE, Hildebrand JG, Tumlinson JH (1989) Pheromone receptor cells in the male moth *Manduca sexta*. Arch Insect Biochem Physiol 10:273–279.
Kaissling KE, Priesner E (1970) Die riechschwelle des seidenspinners. Naturwissenschaften 57:23–28.
Kalidas S, Smith DP (2002) Novel genomic cDNA hybrids produce effective RNA interference in adult *Drosophila*. Neuron 33:177–184.
Keil TA (1989) Fine structure of the pheromone-sensitive sensilla on the antenna of the hawkmoth, *Manduca sexta*. Tissue Cell 21:139–151.
Keil TA, Steinbrecht RA (1984) Mechanosensitive and olfactory sensilla of insects. In: *Insect ultrastructure: volume 2* (King RC, Akai H, eds), pp 477–516. Boston, MA: Springer US.
Krieger J, Klink O, Mohl C, Raming K, Breer H (2003) A candidate olfactory receptor subtype highly conserved across different insect orders. J Comp Physiol A 189:519–526.
Krieger J, Raming K, Dewer YME, Bette S, Conzelmann S, Breer H (2002) A divergent gene family encoding candidate olfactory receptors of the moth *Heliothis virescens*. Eur J Neurosci 16:619–628.
Krishnan B, Dryer SE, Hardin PE (1999) Circadian rhythms in olfactory responses of *Drosophila melanogaster*. Nature 400:375–378.
Kumar S, Stecher G, Li M, Knyaz C, Tamura K (2018) MEGA X: molecular evolutionary genetics analysis across computing platforms. Mol Biol Evol 35:1547–1549.
Laue M, Maida R, Redkozubov A (1997) G-protein activation, identification and immunolocalization in pheromone-sensitive sensilla trichodea of moths. Cell Tissue Res 288:149–158.
Li Y, Song W, Wang S, Miao W, Liu Z, Wu F, Wang J, Sheng S (2024) Binding characteristics and structural dynamics of two general odorant-binding proteins with plant volatiles in the olfactory recognition of *Glyphodes pyloalis*. Insect Biochem Mol Biol 173:104177.
Li J, Wang X, Zhang L (2020) Sex pheromones and olfactory proteins in antheraea moths: a. pernyi and a. Polyphemus (Lepidoptera: Saturniidae). Arch Insect Biochem Physiol 105:e21729.
Linn CE, Campbell MG, Poole KR, Wu W-Q, Roelofs WL (1996) Effects of photoperiod on the circadian timing of pheromone response in male *Trichoplusia ni*: relationship to the modulatory action of octopamine. J Insect Physiol 42:881–891.
Livak KJ, Schmittgen TD (2001) Analysis of relative gene expression data using real-time quantitative PCR and the $2^{-\Delta\Delta\ C(T)}$ method. Methods San Diego Calif 25:402–408.
Loudon C, Koehl MAR (2000) Sniffing by a silkworm moth: wing fanning enhances Air penetration through and pheromone interception by antennae. J Exp Biol 203:2977–2990.
Lundin C, Käll L, Kreher SA, Kapp K, Sonnhammer EL, Carlson JR, von Heijne G, Nilsson I (2007) Membrane topology of the *Drosophila* OR83b odorant receptor. FEBS Lett 581:5601–5604.
Mangmool S, Kurose H (2011) $G_{i/o}$ protein-dependent and -independent actions of pertussis toxin (PTX). Toxins 3:884–899.
Marion-Poll F, Tobin TR (1992) Temporal coding of pheromone pulses and trains in *Manduca sexta*. J Comp Physiol A 171:505–512.
McDonald MJ, Rosbash M (2001) Microarray analysis and organization of circadian gene expression in *Drosophila*. Cell 107:567–578.
Merlin C, Lucas P, Rochat D, François M-C, Maïbèche-Coisne M, Jacquin-Joly E (2007) An antennal circadian clock and circadian rhythms in peripheral pheromone reception in the moth *spodoptera littoralis*. J Biol Rhythms 22:502–514.
Mészáros M, Morton DB (1996) Comparison of the expression patterns of five developmentally regulated genes in *manduca sexta* and their regulation by 20-hydroxyecdysone *in vitro*. J Exp Biol 199:1555–1561.
Miura N, Atsumi S, Tabunoki H, Sato R (2005) Expression and localization of three G-protein α subunits, G_o, G_q, and G_s, in adult antennae of the silkmoth (*Bombyx mori*). J Comp Neurol 485:143–152.
Nakagawa T, Sakurai T, Nishioka T, Touhara K (2005) Insect sex-pheromone signals mediated by specific combinations of olfactory receptors. Science 307:1638–1642.
Nakagawa T, Vosshall LB (2009) Controversy and consensus: noncanonical signaling mechanisms in the insect olfactory system. Curr Opin Neurobiol 19:284–292.
Nakata T, Terutsuki D, Fukui C, Uchida T, Kanzaki K, Koeda T, Koizumi S, Murayama Y, Kanzaki R, Liu H (2024) Olfactory sampling volume for pheromone capture by wing fanning of silkworm moth: a simulation-based study. Sci Rep 14:17879.
Nolte A, Funk NW, Mukunda L, Gawalek P, Werckenthin A, Hansson BS, Wicher D, Stengl M (2013) In situ tip-recordings found no evidence for an orco-based ionotropic mechanism of pheromone-transduction in *Manduca sexta*. PLoS One 8:e62648.
Nolte A, Gawalek P, Koerte S, Wei H, Schumann R, Werckenthin A, Krieger J, Stengl M (2016) No evidence for ionotropic pheromone transduction in the hawkmoth *Manduca sexta*. PLoS One 11: e0166060.

Page TL, Koelling E (2003) Circadian rhythm in olfactory response in the antennae controlled by the optic lobe in the cockroach. J Insect Physiol 49:697–707.
Plautz JD, Kaneko M, Hall JC, Kay SA (1997) Independent photoreceptive circadian clocks throughout *Drosophila*. Science 278:1632–1635.
Riffell JA, Abrell L, Hildebrand JG (2008) Physical processes and real-time chemical measurement of the insect olfactory environment. J Chem Ecol 34:837–853.
Rosén W (2002) Endogenous control of circadian rhythms of pheromone production in the turnip moth, *Agrotis segetum*. Arch Insect Biochem Physiol 50:21–30.
Rosén WQ, Han GB, Löfstedt C (2003) The circadian rhythm of the sex-pheromone-mediated behavioral response in the turnip moth, *Agrotis segetum*, is not controlled at the peripheral level. J Biol Rhythms 18:402–408.
Rymer J, Bauernfeind AL, Brown S, Page TL (2007) Circadian rhythms in the mating behavior of the cockroach, *Leucophaea maderae*. J Biol Rhythms 22:43–57.
Saifullah ASM, Page TL (2009) Circadian regulation of olfactory receptor neurons in the cockroach antenna. J Biol Rhythms 24:144–152.
Sanes JR, Hildebrand JG (1976) Structure and development of antennae in a moth, *Manduca sexta*. Dev Biol 51:282–299.
Sasaki M, Riddiford LM (1984) Regulation of reproductive behaviour and egg maturation in the tobacco hawk moth, *Manduca sexta*. Physiol Entomol 9:315–327.
Sato K, Pellegrino M, Takao N, Tatsuro N, Vosshall LB, Touhara K (2008) Insect olfactory receptors are heteromeric ligand-gated ion channels. Nature 452:1002–1006.
Schendzielorz T, Peters W, Boekhoff I, Stengl M (2012) Time of day changes in cyclic nucleotides Are modified via octopamine and pheromone in antennae of the Madeira cockroach. J Biol Rhythms 27:388–397.
Schendzielorz T, Schirmer K, Stolte P, Stengl M (2015) Octopamine regulates antennal sensory neurons via daytime-dependent changes in cAMP and IP_3 levels in the hawkmoth *Manduca sexta*. PLoS One 10:e0121230.
Schuckel J, Siwicki KK, Stengl M (2007) Putative circadian pacemaker cells in the antenna of the hawkmoth *manduca sexta*. Cell Tissue Res 330:271–278.
Silvegren G, Löfstedt C, Qi Rosén W (2005) Circadian mating activity and effect of pheromone pre-exposure on pheromone response rhythms in the moth *Spodoptera littoralis*. J Insect Physiol 51:277–286.
Sollai G, Solari P, Crnjar R (2018) Olfactory sensitivity to major, intermediate and trace components of sex pheromone in *Ceratitis capitata* is related to mating and circadian rhythm. J Insect Physiol 110:23–33.
Stengl M (1993) Intracellular-messenger-mediated cation channels in cultured olfactory receptor neurons. J Exp Biol 178:125–147.
Stengl M (1994) Inositol-trisphosphate-dependent calcium currents precede cation currents in insect olfactory receptor neurons *in vitro*. J Comp Physiol A 174:187–194.
Stengl M (2010) Pheromone transduction in moths. Front Cell Neurosci 4:133.
Stengl M (2017) Chemosensory transduction in arthropods. In: *The oxford handbook of invertebrate neurobiology* (Byrne JH, ed), New York: Oxford University Press.
Stengl M, Funk NW (2013) The role of the coreceptor orco in insect olfactory transduction. J Comp Physiol A 199:897–909.
Stengl M, Schneider AC (2024) Contribution of membrane-associated oscillators to biological timing at different timescales. Front Physiol 14:1243455.
Stengl M, Schröder K (2021) 14 - Multiscale timing of pheromone transduction in hawkmoth olfactory receptor neurons. In: *Insect pheromone biochemistry and molecular biology*, Ed 2 (Blomquist GJ, Vogt RG, eds), pp 435–468. London: Academic Press.
Stengl M, Zufall F, Hatt H, Hildebrand JG (1992) Olfactory receptor neurons from antennae of developing male *Manduca sexta* respond to components of the species-specific sex pheromone in vitro. J Neurosci 12:2523–2531.
Surguy SM, Duricki DA, Reilly JM, Lax AJ, Robbins J (2014) The actions of *Pasteurella multocida* toxin on neuronal cells. Neuropharmacology 77:9–18.
Tamura K, Nei M (1993) Estimation of the number of nucleotide substitutions in the control region of mitochondrial DNA in humans and chimpanzees. Mol Biol Evol 10:512–526.
Tanoue S, Krishnan P, Krishnan B, Dryer SE, Hardin PE (2004) Circadian clocks in antennal neurons are necessary and sufficient for olfaction rhythms in *Drosophila*. Curr Biol 14:638–649.
Thamm M, Scholl C, Reim T, Grübel K, Möller K, Rössler W, Scheiner R (2017) Neuronal distribution of tyramine and the tyramine receptor AmTAR1 in the honeybee brain. J Comp Neurol 525:2615–2631.
Tumlinson JH, Brennan MM, Doolittle RE, Mitchell ER, Brabham A, Mazomenos BE, Baumhover AH, Jackson DM (1989) Identification of a pheromone blend attractive to *Manduca sexta* (L.) males in a wind tunnel. Arch Insect Biochem Physiol 10:255–271.
Ueno K, Kohatsu S, Clay C, Forte M, Isono K, Kidokoro Y (2006) Gsα Is involved in sugar perception in *Drosophila melanogaster*. J Neurosci 26:6143–6152.
Vosshall LB, Amrein H, Morozov PS, Rzhetsky A, Axel R (1999) A spatial map of olfactory receptor expression in the *Drosophila* antenna. Cell 96:725–736.
Vosshall LB, Hansson BS (2011) A unified nomenclature system for the insect olfactory coreceptor. Chem Senses 36:497–498.
Wegener JW, Hanke W, Breer H (1997) Second messenger-controlled membrane conductance in locust (*Locusta migratoria*) olfactory neurons. J Insect Physiol 43:595–603.
Wetzel CH, Behrendt H-J, Gisselmann G, Störtkuhl KF, Hovemann B, Hatt H (2001) Functional expression and characterization of a *Drosophila* odorant receptor in a heterologous cell system. Proc Natl Acad Sci U S A 98:9377–9380.
Wicher D, Miazzi F (2021) Functional properties of insect olfactory receptors: ionotropic receptors and odorant receptors. Cell Tissue Res 383:7–19.
Wicher D, Morinaga S, Halty-deLeon L, Funk N, Hansson B, Touhara K, Stengl M (2017) Identification and characterization of the bombykal receptor in the hawkmoth *Manduca sexta*. J Exp Biol 220:1781–1786.
Wicher D, Schäfer R, Bauernfeind R, Stensmyr MC, Heller R, Heinemann SH, Hansson BS (2008) *Drosophila* odorant receptors are both ligand-gated and cyclic-nucleotide-activated cation channels. Nature 452:1007–1011.
Wistrand M, Käll L, Sonnhammer ELL (2006) A general model of G protein-coupled receptor sequences and its application to detect remote homologs. Protein Sci Publ Protein Soc 15:509–521.
Yao CA, Carlson JR (2010) Role of G-proteins in odor-sensing and CO_2-sensing neurons in *Drosophila*. J Neurosci 30:4562–4572.
Zhu MX (2023) High resolution cryo-EM structures of TRPC5-$G\alpha_{i3}$ complexes reveal direct activation of an ion channel by $G\alpha_i$-GTP. Cell Calcium 113:102767.
Zhukovskaya MI (1995) Circadian rhythm of sex pheromone perception in the male American cockroach, *Periplaneta americana* L. J Insect Physiol 41:941–946.
Ziegelberger G, van den Berg M, Kaissling KE, Klumpp S, Schultz JE (1990) Cyclic GMP levels and guanylate cyclase activity in pheromone-sensitive antennae of the silkmoths *Antheraea polyphemus* and *Bombyx mori*. J Neurosci 10:1217–1225.